Surface-field-induced effects on morphologies of lamella-forming diblock copolymers in nanorod arrays*

Wang Xiang-Hong(王向红)[a)b)†], Li Shi-Ben(李士本)[b)], Zhang Lin-Xi(章林溪)[b)], and Liang Hao-Jun(梁好均)[c)]

[a)] *Department of Physics, Wenzhou Vocational and Technical College, Wenzhou* 325035, *China*

[b)] *Department of Physics, Wenzhou University, Wenzhou* 325035, *China*

[c)] *Department of Polymer Science and Engineering, University of Science and Technology of China, Hefei* 230026, *China*

(Received 3 December 2010; revised manuscript received 18 March 2011)

The surface-induced effect on the morphologies of lamella-forming diblock copolymers in nanorod arrays is studied by using the self-consistent field theory. In the simulation study, a rich variety of novel morphologies are observed by variations in the strength of the surface field for the diblock copolymers. Different surface-field-induced effects are examined for the diblock copolymers in the arrays with distinct preferential surfaces. It is observed that the majority-block preferential surfaces have more obvious induced effects than those of minority-block preferential surfaces. The strong surface fields exhibit different behaviours from those observed in the weak surface fields, by which the morphologies possess cylindrical symmetries. Results from this research deepen the knowledge of surface-induced effects in a confinement system, which may aid the fabrication of polymer-based nanomaterials.

Keywords: diblock copolymer, surface-induced effect, morphology, nanorod array

PACS: 36.20.–r, 61.25.hk, 64.70.kmj **DOI:** 10.1088/1674-1056/20/8/083601

1. Introduction

Linear AB diblock copolymers exhibit a rich variety of self-assembled morphologies in bulk due to the repulsed interactions between their two different blocks. These morphologies include typical phases, such as lamellar, cylindrical and spherical phases, as well as a series of complicated bicontinuous phases, which have been recently reported.[1−3] Restricted by the length of blocks, the self-assembled morphologies of diblock copolymers are on nanoscales, which facilitates the fabrication of nanomaterials in a wealth of potential nanotechnology applications, including lithography and laser devices.[4,5] Since a confinement environment naturally exists in the block copolymer system, its surface field or preferential surface, along with its geometric shape, should be taken into account in a confined system.[6] In addition to the geometric shapes, the surface field plays a basic role in contributing the required enthalpy energy to the system during the introduction of the confinement surfaces; this aspect has attracted increasing interest over the previous decade.

Diblock copolymer thin films, i.e., diblock copolymers confined between two parallel walls, have received a large number of contributions in the experimental and theoretical fields, and also in the simulation field.[7−24] Specifically, bulk lamellae can be induced into the mixed structure: a structure with two components of lamellae placed parallel and perpendicular to the confined surfaces when the thin film has strongly asymmetric surfaces.[23−25] It showed that the strengths of surface fields or the surface tensions are crucial to the formation of these mixed lamellae. Furthermore, diblock copolymers can be induced into desired morphologies since the thin film has special

*Project supported by the National Natural Science Foundation of China (Grant Nos. 20374050, 20934004, 21074096, 50773072, and 90403022), the Outstanding Youth Fund of China (Grant No. 20525416), the National Basic Research Program of China (Grant No. 2005CB623800), Program for New Century Excellent Talents in University (Grant No. NCET-05-0538), the Natural Science Foundation of Zhejiang Province (Grant Nos. Y4090174 and Y6100033), and the Science Technology Development Plan of Wenzhou City, China (Grant No. H20080041).

†Corresponding author. E-mail: wxh@wzvtc.cn

© 2011 Chinese Physical Society and IOP Publishing Ltd

patterned surfaces.[11,23,26] In the studies reported in the literatures, surfaces have been reported to have a strong preference to one type of block and patterns have periodic characteristics such that these surfaces can be considered as an ideal template. In recent times, many studies have contributed to the advancement in diblock copolymers confined in cylindrical nanopores — a confinement surface with cylindrical symmetry.[27−45] These studies have usually researched the surface fields and confinement sizes based on characterization by pore diameters. For example, Liang *et al.* investigated morphological dependences on the strength of surface fields by using a Monte Carlo (MC) simulation.[33] In their study, symmetric (i.e. lamella-forming) diblock copolymers were adopted in the strong segregation regime and several special morphologies, such as stacked-disk and single helix structures, were observed when the strength of surface fields was increased for various pore diameters. Li *et al.* investigated the effects of surface preference and pore diameter on the morphologies of symmetric diblock copolymers confined in nanopores by using MC simulations,[42] in which a rich variety of morphologies, including the parallel lamellae, perpendicular lamellae and cylindrically concentric lamellae, were investigated for the symmetric diblock copolymers. The cylinder-forming diblock copolymers exhibited more complicated morphologies and phase behaviours as the surface preference was varied for the various pore diameters.[39,40,42,43] Under nanopore confinements, the bulk cylinders are forced into a series of distorted morphologies, such as a double helix and perforated tubes, due to cylindrical symmetries originating from the confinement surface. When diblock copolymers are confined in a spherical space, confinement requires that they can be packed into a crowded environment, leading to other types of morphologies.[27,46−53] Usually, the lamella-forming diblock copolymers in a spherical space can self-assemble into morphologies with spherical symmetries while the cylinder-forming ones have strong body-centred symmetries with multilayered structures.[46,51,52] There is evidence that the morphologies gained from thin film, nanopore and spherical confinements can be understood based on the match between the confinement sizes and bulk polymer periods, as well as by the symmetric requirement of confinement surfaces.

However, thin film, cylindrical nanopore and spherical confinement are provided by the inner surfaces of confinement boundaries. In recent times, we investigated the morphologies of diblock copolymers confined in nanorod and nanoparticle arrays where confinements are provided by the outer surfaces of the nanorods or nanoparticles.[54−56] For nanoparticle-array confinement, we investigated order–disorder and order–order phase transitions in the arrays with large and small periods, respectively, when the strengths of the surface field engendered on the nanoparticles were augmented with small, stepped increments for various diameters.[56] These morphologies were found to have mono- or bicontinuous structures, with cubic symmetries, in the nanoparticle arrays which are mainly attributable to cubic symmetries from the nanoparticle arrays. For nanorod-array confinements, the array period plays an important role in inducing morphologies although they almost have similar cylindrical symmetries. In arrays with small periods, monolayered structures prevail while multi-layered structures appear in the arrays with large periods.[54,55] We observed several continuous phases of diblock copolymers in the nanorod arrays with small periods by varying the strength of the surface fields. Alternatively, we focused on the confinement-induced effect of nanorod arrays on the morphologies of diblock copolymers in large period arrays and complicated bicontinuous structures have been observed for several large nanorod arrays with individual values of surface fields.[55] In the present work, we extend the results from our previous works and explore the mechanism by which the surface field affects the morphologies of diblock copolymers in nanorod arrays with large periods. Novel morphologies are expected to be observed for diblock copolymers confined in such a system when the strength of surface fields is varied. In Section 2, we outline the experimental model and calculation method, the results and discussion are presented in Section 3. Conclusions drawn from our finding are presented in Section 4.

2. Model and method

The model consists of two parts: the model polymer and the nanorod array. We selected the model polymer to be a lamella-forming diblock copolymer, as shown in Fig. 1(a).

The diblock copolymers are regarded as Gaussian chains with the volume fraction of A-blocks, f_{A} and polymerization index N. The diblock copolymer has

the same statistical length, b, and, subsequently, the radius of gyration $R_g^2 = Nb^2/6$. The repulsion interactions between the A and B blocks are parameterized with χN where χ is the Flory–Huggins parameter. In the present work, we specified polymer parameters as $f_A = 0.4$ and $\chi N = 0.4$, having a bulk polymer period of $L_0 = 4.4R_g$, which are similar to the specifications applied in our previous work.[54,55] The advantage of this choice is not only that it provides an opportunity for comparison with the previous works, but also that the slightly asymmetric block enables comparison of different surface preferences. Furthermore, the nanorod-array model is presented in Fig. 1(b), in which only the cross section of the array is plotted in the x–y plane with the period L_x and L_y in the x and y directions, respectively. The nanorod array is composed of periodically arranged nanorods with solid and impermeable surfaces, having infinite length and diameter D. A calculation unit with the periodic boundary condition (the zone with dotted lines) is introduced to construct the entire array in the simulation, as shown in Fig. 1(c). The match between the bulk polymer period and the periodic boundary condition is crucial to avoid an artificial microstructure in a system of infinite size.[25] In order to avoid this, we select $L_z = 2L_0$ to construct the infinite length in the z axis; and select $L_x = L_y = 3L_0$ to construct the infinite size in the x and y axes for the infinite length array, as shown in Fig. 1(c).

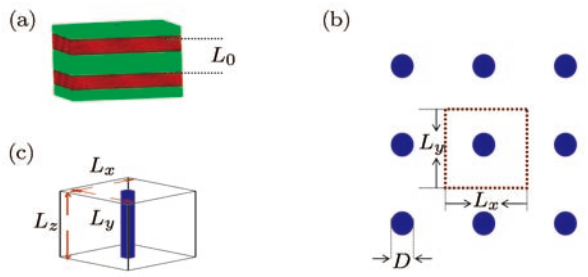


Fig. 1. Schematic illustration of lamella-forming diblock copolymers with bulk period L_0 in nanorod array. (a) The lamella-forming diblock copolymers with bulk period of L_0. (b) The periodic nanorod array is shown with its cross section in the x–y plane. Here, D denotes the diameter of nanorod, L_x and L_y represent the array periods in the x and y directions, respectively. The zone with dotted lines represents the calculation unit. (c) The calculation unit in three dimensions.

Based on a Gaussian chain model, the self-consistent field theory (SCFT) has been proven to be a powerful tool for exploring the novel morphologies of block copolymers. For diblock copolymers in an external field, the free energy per chain can be expressed in units of k_BT for the volume V[40,57] as

$$\begin{aligned}\frac{F}{nk_BT} = &-\ln\left(\frac{Q}{V}\right) + \frac{1}{V}\int \mathrm{d}r[\chi N\phi_A\phi_B \\ &-\omega_A\phi_A - \omega_B\phi_B - U_A\phi_A - U_B\phi_B \\ &-P(\phi_0 - \phi_A - \phi_B)]. \end{aligned} \quad (1)$$

Here, $\phi_{A(B)}$ is the corresponding monomer density field normalized by the local volume fractions of the blocks, $\omega_{A(B)}$ is the mean field originating from the repulsion interactions between A- and B-blocks, while P is a Lagrange multiplier that ensures the incompressibility of the system. We generalize the incompressibility constraint to $\phi_A + \phi_B = \phi_0$ and set $\phi_0 = 0$ on the lattices inside solid rods, $\phi_0 = 0.5$ for the lattice next to the outer surfaces of the rods and $\phi_0 = 1.0$ elsewhere. $U_{A(B)}$ is always non-negative and denotes the strength of the surface field, which reflects the short-range surface–polymer interactions between the nanorod surfaces and A(B) blocks located on the lattices next to the surfaces. Therefore, $U_{A(B)}$ is only applied to the lattices next to the surfaces outside the rods. Furthermore, we reduced the strength of the surface field to $\lambda_{a(b)} = U_{A(B)}/\chi N$. The single chain partition function, Q, can be expressed as $Q = \int q(\boldsymbol{r}, 1)\mathrm{d}r$ in the mean field $\omega_{A(B)}$. The segment distribution function, $q(\boldsymbol{r}, s)$, is the statistical weight of a chain segment of contour length s containing a free chain end and with its connected end located at $\boldsymbol{r}$, which satisfies the modified diffusion equation in the mean fields, that is,

$$\frac{\partial}{\partial s}q(\boldsymbol{r}, s) = R_g^2\nabla^2 q(\boldsymbol{r}, s) - N\omega q(\boldsymbol{r}, s)$$

with the initial condition of $q(\boldsymbol{r}, 0) = 1$. Alternatively, another segment distribution $q'(\boldsymbol{r}, s)$ is necessary, which satisfies the modified diffusion equation multiplied by -1 on the left-hand side of the equation and with the initial condition of $q'(\boldsymbol{r}, 1) = 1$.

The free energy is minimized to a stable value with respect to the mean fields and the segment density fields in order to obtain the equilibrium phase. The minimization of free energy results in a set of self-consistent equations, which can be expressed as

$$\omega_A(\boldsymbol{r}) = \chi(\phi_B(\boldsymbol{r}) - f_B) - U_A(\boldsymbol{r}) + P(\boldsymbol{r}), \quad (2)$$

$$\omega_B(\boldsymbol{r}) = \chi(\phi_A(\boldsymbol{r}) - f_A) - U_B(\boldsymbol{r}) + P(\boldsymbol{r}), \quad (3)$$

$$\phi_A(\boldsymbol{r}) = \frac{V}{Q}\int_0^{f_A} dsq(\boldsymbol{r}, s)q'(\boldsymbol{r}, s), \quad (4)$$

$$\phi_{\mathrm{B}}(\boldsymbol{r}) = \frac{V}{Q}\int_{f_{\mathrm{A}}}^{1} ds q(\boldsymbol{r}, s) q'(\boldsymbol{r}, s). \quad (5)$$

To solve the above SCFT equations, we use a combinatorial screening method based on the real-space implementation, which was originally proposed by Drolet and Fredrickson.[58] In the real-space implementation, a relaxation process with iteration steps is assumed to search the equilibrium morphology until the free energy of system is minimized to a stable value. The real-space SCFT has been successfully used to obtain the morphologies of the multi-block copolymers without requiring assumptions about the symmetry of the system.[57] During calculations, the free energy criterion is that the free energy difference between two sequential iteration steps should be less than 1.0×10^{-11}. Moreover, each minimization of the free energies is run several times by using different random initial mean fields ω_{A} and ω_{B} to ensure that the exact equilibrium morphology has been obtained. In the present study, we consider $0.2R_{\mathrm{g}}$ as the lattice size and divide the chain contour length into 200 monomers, which is similar to that applied in our previous works.[40,54,59] The SCFT calculations are performed in a PC cluster with 25 crunodes.

3. Results and discussion

In order to examine how the surface field affects the morphologies of diblock copolymers confined in nanorod arrays, we selected several arrays with typical nanorod diameters and increased the strength of surface field $\lambda_{\mathrm{a(b)}}$ from zero to one, a degree comparable with the interaction among the blocks themselves, with steps of $\Delta\lambda_{\mathrm{a(b)}} = 0.05$. In the present work, we consider three cases, the small nanorod case of $D/L_0 = 0.09$, the moderate-sized rod case of $D/L_0 = 0.62$ and the large rod cases of $D/L_0 = 1.21$ and $D/L_0 = 1.91$, respectively. The morphologies observed in the arrays are presented in the form of three different colours (red, green and blue), which represent the density distributions of the monomers belonging to A-block, B-block and nanoparticles, respectively. The surface-induced morphologies are shown in Figs. 2–4, along with their denominations and the corresponding values of $\lambda_{\mathrm{a(b)}}$. In addition, the structures are only drawn by either A-blocks or B-blocks, or their cut views, in order that they are observed in a visible manner.

3.1. Arrays with small nanorods

We consider the diblock copolymers in the nanorod array with $D/L_0 = 0.09$, an array with small rods, and investigate surface-induced effects on their morphologies, as depicted in Fig. 2. Only three types of morphologies were observed in the arrays with small nanorods and the A-preferential surfaces. First, we observed the parallel lamellae (denoted as PAL) in such an array in the absence of a surface field. The PAL morphologies are similar to the bulk lamellae, indicating that we can ignore the influence of the array confinement on the morphologies. We also observed PAL structures in nanorod arrays with other parameters where the array period is selected to be the polymer period.[54] Certainly, the nanorod diameter of $D/L_0 = 0.09$ is too small to affect the morphologies in arrays with either large or small periods. It is desirable to investigate the effects of surface fields on such small rods when the strength of the surface field is increased. As expected, a complicated structure was observed over a range of $\lambda_{\mathrm{a}} = 0.05$–$0.85$, as shown in Fig. 2(a2). To describe this structure clearly, we divide this structure into the inner and outer zones in the calculation unit. In the B-block matrix, the A-blocks assemble into a continuous network with double-layered structures: one layer is close to the edge of the unit while the other has a rhombic mesh structure between two circular structures. Conversely, the B-blocks exhibit an irregularly continuous cylindrical network in the inner zone and perpendicular cylinders in the outer zone. For the entire nanorod array, we subsequently observed a bicontinuous network along with the cylinders (denoted as BN1-C structure). This complicated bicontinuous network accompanied by cylinders differs from the network phase with an orthorhombic structure observed in the bulk system.[2,3] The BN1-C network has the same symmetry as the nanorod array because of confinement-induced effects. Such a BN1-C structure transits into a relatively simple structure when the strength of surface field is increased to a relatively strong range, i.e. $\lambda_{\mathrm{a}} = 0.90$–$1.00$. As shown in Fig. 2(a3), we observed the PAL once again in the outer zone. We noted the appearance of a cylindrical lamella (CL) constructed by double layers in the inner zone. This CL structure is due to the strong adsorption effect of the surface field with respect to its cylindrical symmetry. Actually, such a cylindrical lamella has been reported for diblock copolymers confined in nanopores in experiment[29] and MC simulations.[27,42]

The dependence of CL thickness on the pore diameter has been predicted for multilayered structures.[42] In this instance, we observed only the CL structure with double layers since the surface field is not strong enough for strength and the nanorod is too small for its diameter. However, it is reasonable to conclude that the multilayered CL structure in the nanorod array will be observed in an array with a large period and strong surface field. Therefore, the diblock copolymers assemble into a CL–PAL structure in the entire array. This CL–PAL structure has been observed in nanorod arrays with a neutral surface and a relatively large rod diameter ($D/L_0 = 0.21$–0.27), indicating that increasing the strength of the surface field is equivalent to increasing the nanorod diameter.[55]

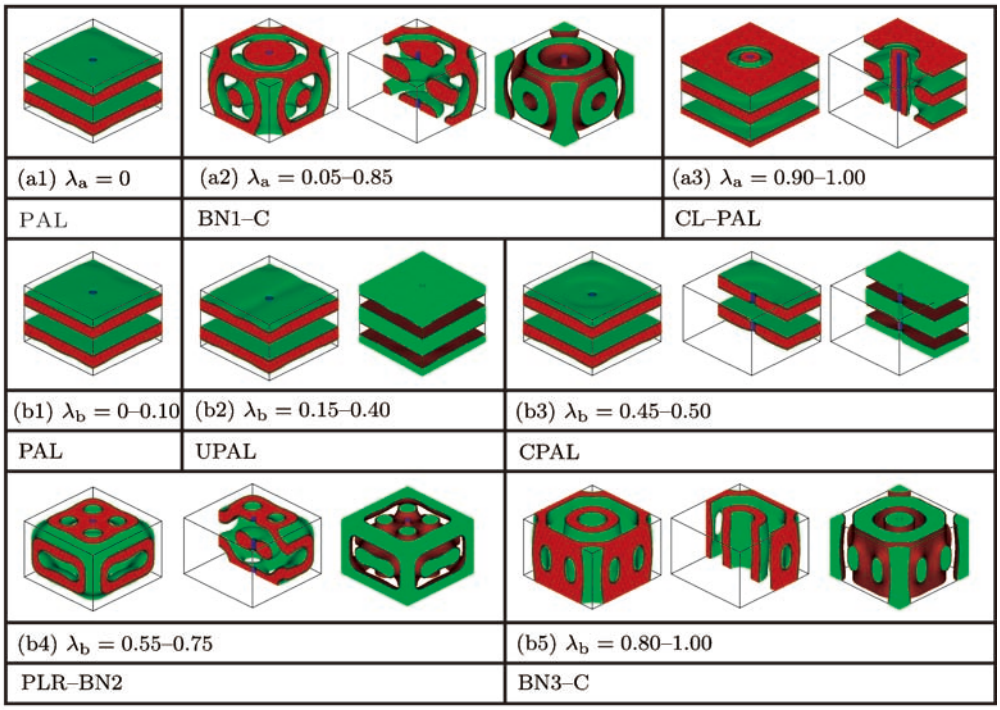


Fig. 2. Morphological dependences of lamella-forming diblock copolymers on the strength of surface field $\lambda_{a(b)}$ for the arrays with $D/L_0 = 0.09$. The values of $\lambda_{a(b)}$ and denotations of morphologies are listed below the structures. The red, green and blue colours represent A-blocks, B-blocks and nanorods, respectively.

The slightly asymmetric blocks of the model polymers enable us to compare the different effects of surface fields on the major (B-) and minor (A-) blocks. For the B-preferential surfaces, figure 2(b) depicts an evolvement process with the strength of the surface field. First, we observed a perfect PAL structure at a weak surface field of $\lambda_b = 0.00$–0.10 [see Fig. 2(b1)]. Then, the PAL structure evolved into a slightly undulating PAL (denoted as UPAL structure) over a wide range of $\lambda_b = 0.15$–0.40 [see Fig. 2(b2)] and, subsequently, into circularly undulated PAL (CPAL) at $\lambda_b = 0.45$–0.50, where the undulated patterns are circular around the nanorods [see Fig. 2(b3)]. In this evolvement process, although there is a negligible variation in pattern with increasing λ_b, the diblock copolymers still maintain the flat characteristic of PAL. Specifically, the circular undulation appears at $\lambda_b = 0.45$–0.50 because of the relatively strong surface field with cylindrical symmetry. For $\lambda_b = 0.00$–0.10, the surface field is too weak to influence the lamellar patterns, while the surface field with cylindrical symmetry is not strong enough to adsorb the majority blocks around the nanorod with cylindrical distribution, such that the contradiction between the cylindrical symmetry and flat characteristic of the PAL structure results in the UPAL structure. The UPAL structure has been observed in nanorod arrays with small periods where the undulated orientation is along the nanorod due to adsorption effects along the rods.[54] Here, the undulation orientation of UPAL is perpendicular to the nanorod. However, with continuously increasing λ_b, the lamellar structure transits

into a complicated PCR–BN2 structure, at $\lambda_b = 0.55$–0.75 [see Fig. 2(b4)]. In the B-block matrix, two perforated lamellae with A-block layers are packed into a cubic structure, along with a ring inside the cube (PLR). Perforated lamellae have been extensively reported for the diblock copolymers in thin film.[13−15] Here, we observed another type of perforated lamellae, the PLR structure. From the viewpoint of B-blocks, there is a cubic network in the outer zone while an irregular lamella with four cylinders is in the inner zone, resulting in a bicontinuous network (BN2). It should be pointed out that this BN2 is composed of only B-blocks and differs from the BN1 network that is formed by two types of blocks. Finally, under the strong surface field, the PLR–BN2 transits into a structure with a type of cylindrical symmetry, the BN3–C structure [see Fig. 2(b5)]. It is logical that the strong surface field adsorbs major blocks into the nanorods with cylindrical symmetry, leading to a cylindrical A-block lamellae near the nanorods in the inner zone and four solid B-block cylinders in the outer zone. The remaining parts then form a bicontinuous network structure (denoted as the BN3 structure), so as to constitute the BN3–C structure in the whole array.

It is worth while here to summarize several general characteristics of surface-induced morphologies of diblock copolymers in arrays with small nanorods. First, diblock copolymers have different behaviours in weak and relatively strong surface fields. Usually, the diblock copolymers maintain the bulk PAL structure in the weak surface field while the structures with cylindrical symmetry appear in relatively strong surface fields in order to meet the cylindrical symmetries from the surface field. Then, difference-induced effects can be observed in the A- and B-preferential surfaces. Specifically, morphologies induced by B-preferential surfaces are more complicated than those induced by A-preferential surfaces. We only observed three types of structures, PAL, BN1–MC, and CL–PAL structures, in the A-preferential surfaces while PAL, UPAL, CPAL, PLR–BN2, and BN3–C structures are observed in the B-preferential surfaces. Thus, these differences arise from the slight asymmetry around the blocks.

3.2. Arrays with moderate-sized nanorods

The confinement size and shape are crucial to self-assembled morphologies of diblock copolymers in inner-surface-confinement cases.[60] It is expected that surface-induced effects on the morphologies of diblock copolymers under the outer surface confinements may be observed with different confinement sizes. In this subsection, we report the investigation of morphological dependences on the strength of surface field $\lambda_{a(b)}$ for arrays with $D/L_0 = 0.62$, the arrays with moderate-sized nanorods, as shown in Fig. 3.

First, we observed a structure, the CL–LN1 structure, with a monolayer of CL in the inner zone and a square lamella connecting the neighbouring lamellae, resulting in an irregular lamellar network (LN1) structure in the outer zone. This CL–LN1 structure occurs in the absence of a surface field and maintains its pattern in the weak surface field [see Fig. 3(a1)]. Although we have observed a similar CL–LN1 structure in nanorod arrays with neutral surfaces in our previous work,[55] the result indicates that the CL–LN1 structure is insensitive to the weak surface field. However, when the surface field is strengthened to a suitable degree, the CL–LN1 structure develops into another lamellar network structure with an unchanged CL layer, the CL–LN2 structure, at $\lambda_a = 0.40$–0.65 [see Fig. 3(a2)], where there are four cylinders perforating the lamellar network from the outer zones (LN2 structure). Then, with increasing λ_a, the connectivity between the neighbouring layers is strengthened in the outer zone over a range of $\lambda_a = 0.70$–0.90 [see Fig. 3(a4)] and passes through an intermediate morphology at $\lambda_a = 0.75$ [see Fig. 3(a3)], which then brings about the complete continuity of the lamellar network at $\lambda_a = 1.00$ [see Fig. 3(a5)]. To elucidate, the transition sequence is from CL–BN3 to CL–BN4 and then to SL–BN5 with increasing λ_a. It should be pointed out that, although the lamella network structure changes its pattern in the outer zone during the evolvement process, it still retains the bicontinuous characteristic, i.e. BN3, BN4 and BN5. It should be noted here that a similar evolvement process has been reported in our previous work where the array has neutral surfaces and the diameter is increased.[55] Our present observation indicates that the surface-induced effect can be made equivalent to

that of the confinement-induced effect by varying the nanorod diameter. Actually, the cylindrical symmetry is strengthened with increasing λ and, subsequently, the cylindrical lamellae are fastened. However, since the surface field is short ranged, the outer zone still maintains the square symmetry and the difference of symmetry in the inner and outer zones results in an evolvement process.

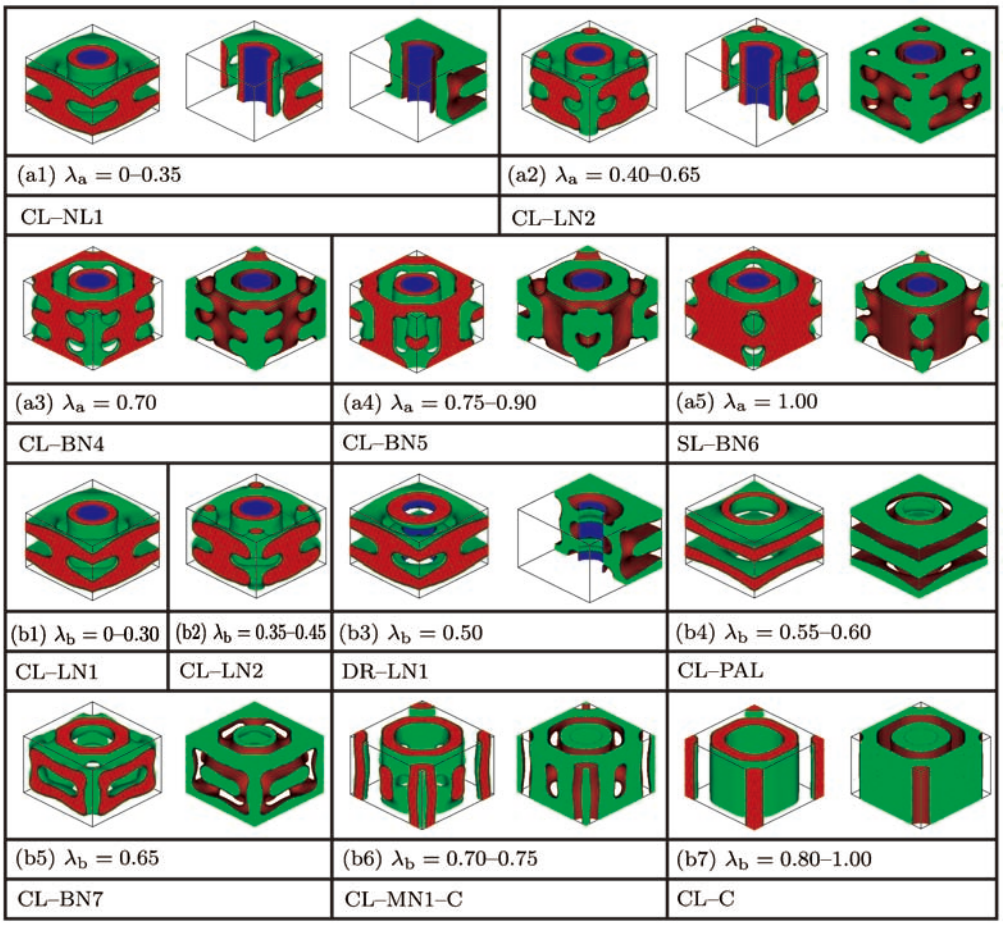


Fig. 3. Morphological dependences of lamella-forming diblock copolymers on the strength of surface field $\lambda_{a(b)}$ for the arrays with $D/L_0 = 0.62$. Here, The values of $\lambda_{a(b)}$ and denotations of morphologies are listed below the structures. The red, green and blue colours represent A-blocks, B-blocks and nanorods, respectively.

For the B-preferential surfaces, the diblock copolymers maintain the CL–LN1 mixture structure at λ_b = 0–0.30 [see Fig. 3(b1)] and, subsequently, transit into a CL–LN2 structure at λ_b = 0.35–0.45 [see Fig. 3(b2)]. This evolvement process is similar to the observation in the case of surface preferences to minority blocks, as shown in Fig. 3(a1) and 3(a2). A slight difference is that a wider range of λ_a is required to be applied on the surface than those of λ_b, since the slightly asymmetric blocks require the major block to have more adsorption energies than those of minority blocks at the same value of surface field. Then, the CL–LN2 structure transits into an intermediate structure at λ_b = 0.50 (DR–LN1 structure), with double rings (DR) in the inner zone and lamellar network (LN1) in the outer zone [see Fig. 3(b3)]. This CL–LN2 structure subsequently develops into several similar structures with increasing λ_b, with the unchanged CL structure in the inner zone, as shown in Figs. 3(b4)–3(b7). At the first stage, the diblock copolymers assemble into the structure with the CL layer in the inner zone and PAL structure in the outer zone [CL–PAL structure], as shown in Fig. 3(b4). It is notable that, although this CL–PAL structure is similar to that observed in Fig. 2(a3), the difference is obvious: the CL structure is constructed by the inner B-block layers with larger diameter, due to the relatively strong B-preferential surfaces. This fact reinforces the fact that the fabrication of a similar structure with reversed blocks in nanotechnology for a desired purpose. When the strength of the surface field is increased to λ_b = 0.65, the CL–PAL structure evolves into another intermediate structure, the CL–BN7 structure, where there is an irregular CL layer in the inner zone

while the bicontinuous network appears in the outer zone [see Fig. 3(b5)]. This intermediate structure was only observed at a very narrow range and quickly transited into the second stage [see Figs. 3(b6) and 3(b7)]. This stage exhibits an outstanding characteristic of the four cylinders appearing in the outer zone. Specifically, there are cylinders with double layers at $\lambda_b = 0.70$–0.75 and with single A-block layer at $\lambda_b = 0.80$–1.00 in the outer zone. Similarly, these cylinders originate from the strong B-preferential surface that requires the structures to have more cylindrical symmetry in the system. Under the thin film or cylindrical nanopore confinements, the strength of the surface field mainly changes the orientation of parallel layers[25,29] or numbers of cylindrical layers.[41,42] However, the surface-field-induced effects on the morphologies of diblock copolymers in nanorod arrays are quite different from those in thin-film and cylindrical nanopore confinements, in which the morphologies can be drastically reorganized by increasing λ_b.

There are several general characteristics surrounding the evolvement in comparison with the small nanorod case. First, the cylinders in the outer zones, either with double layers or a single solid layer, can be observed in the strong B-preferential surface fields, other than the strong A-preferential surface fields. The reason is probably due to the slight asymmetry about the blocks. As pointed out earlier, the B-preferential surface field contributes more adsorption energies to the system than those of A-preferential surface fields and, therefore, it is easier to assemble into cylinders at the same value of the surface field. Secondly, we observed the same complicated evolvement in the A-preferential surface fields at the moderate diameter case, unlike at the small nanorod case, which may have been caused by nanorods with moderate diameters. The relatively large diameter of a nanorod provides additional adsorption energy, leading to the complicated evolvement in the moderate-sized nanorod case.

3.3. Arrays with large nanorods

In this subsection, we report results of our investigation of morphological dependences on the strength of the surface field $\lambda_{a(b)}$ for arrays with large nanorods of $D/L_0 = 1.21$, as shown in Fig. 4, and with the large nanorods of $D/L_0 = 1.91$, shown in Fig. 5, respectively. For $D/L_0 = 1.21$ and $D/L_0 = 1.91$, nanorods occupy 12.66% and 31.82% of the total volume in the whole arrays, respectively, such that their volume occupancy is drastically increased from 0.07% in the small nanorod case to 3.35% in the moderate-sized nanorod case. We expected to observe the distinguished morphologies of diblock copolymers under such severe confinements.

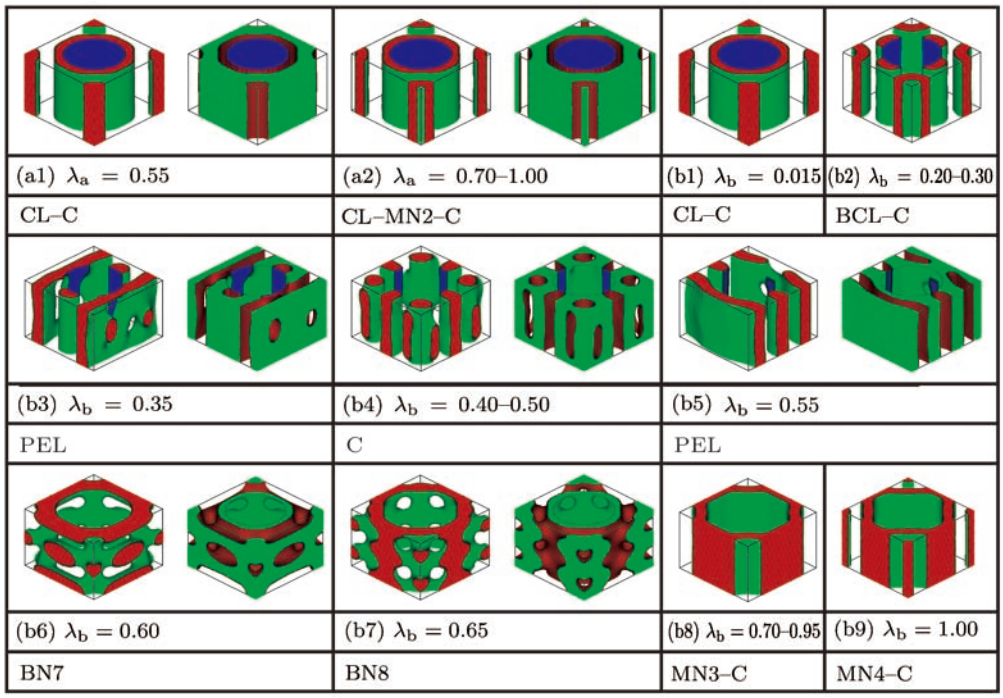


Fig. 4. Morphological dependences of lamella-forming diblock copolymers on the strength of surface field $\lambda_{a(b)}$ for the arrays with $D/L_0 = 1.21$. Here, The values of $\lambda_{a(b)}$ and denotations of morphologies are listed below the structures. The red, green and blue colours represent A-blocks, B-blocks and nanorods, respectively.

In nanorod arrays with neutral surfaces and $D/L_0 = 1.21$, diblock copolymers assemble into the CL–C structure, where the concentric lamellae are in the inner zone and four solid cylinders in the outer zone. With increasing λ_a, we observed that diblock copolymers maintain the CL–C structure over a relatively wide range of $\lambda_a = 0$–0.55 [see Fig. 4(a1)]. This CL–C structure is similar to the microstructure reported in our previous work.[55] Due to the large confinement surface, the weak field imposed on the surface can obviously affect the CL–C structure. As we expected, in order to meet the requirement of the cylindrical symmetry of surface field, the major component becomes the mono-continuous network (MN2) structure in the inner zone when the strength of surface field is increased to $\lambda_a = 0.60$–1.00 [Fig. 4(a2)]. Thus, we observed the CL–MN2–C mixture structure at a relatively strong surface field. For the A-preferential surfaces, only two structures take part in the evolvement process, similar to the evolvement process observed in arrays with small periods where the severe confinement was also considered.[54] Usually, surface-induced effects on severe confinements, such as pore and sphere confinement with small diameters, cause a relatively simple morphological transformation.[42,43,51] For example, there are only a few structures, such as parallel and cylindrical lamellae, which take part into the transformation process with increasing surface field strength.[42] In these processes, the symmetries of morphologies commonly change to accommodate the surface field. However, the present observation indicates that the above evolvement observed in Figs. 4(a1) and 4(a2) maintains invariable cylindrical symmetry in the process, which is probably attributable to the short-ranged surface field and the outer surface confinement provided by nanorods.

Imposing the B-preferential surface field, we find that a rich variety of microstructures were observed with increasing λ_b. Unlike in the case of the A-preferential surface, the slight increase in λ_b can destroy the CL–C structure such that diblock copolymers maintain their structure only at a quite narrow range of $\lambda_b = 0$–0.15 [Fig. 4(b1)]. This insensitivity of λ_b to the CL–C structure indicates that the surface preference for major blocks is crucial to the evolvement process. With increasing λ_b, the concentric lamellae are broken at four positions because B-block components are adsorbed into the nanorods (BCL) while the cylinders with double layers appear in the outer zone, so that we observed the BCL–C structure at a narrow range of $\lambda_b = 0.20$–0.30 [see Fig. 4(b2)]. For $\lambda_b = 0.35$, the broken concentric lamellae graft on cylinders and evolve into the perpendicular lamellar (PEL) structure [Fig. 4(b3)]. We note that this structure has also been observed in another type of arrays with surface preference to the major block at the confinement dimension $d = 0.45$.[54] Given that nanorod periods are three times that of the polymer periods, three layers of PEL appear in the calculation unit. In other words, the period of the PEL structure is the same as that of the polymer period, which is similar to that reported in our previous work.[54] At $\lambda_b = 0.40$–0.50, we observed that the PEL are broken into the discontinuous PEL [DPEL structure], which is analogous to cylindrical arrays, as shown in Fig. 4(b4). It is surprising that the PEL structure appears again at $\lambda_b = 0.55$ [Fig. 4(b5)]. The PEL and DPEL structures are observed in a very narrow range of surface field, reflecting that these microstructures are very sensitive to the strength of the surface field. Then, the diblock copolymers develop into a series of continuous structures with increasing λ_b. Specifically, diblock copolymers transit into an irregular bicontinuous network (BN7) structure at $\lambda_b = 0.60$ and quickly transit into another bicontinuous network at $\lambda_b = 0.65$ (BN8), with stronger connectivity between them [see Fig. 4(b7)]. Subsequently, the strong surface field requires that diblock copolymers have similar symmetry so that irregular bicontinuous networks disappear in the array and the regular structure emerges at such surface field. Therefore, we observed a monocontinuous network (MN3) structure, along with the cylinders (C), at $\lambda_b = 0.70$–0.95, in which the minor blocks exhibit the lamellar characteristic and connect with each other in neighbouring units. On the other hand, the major blocks assemble into the concentric lamella with a monolayer in the inner zone and four solid cylinders in the outer zone [see Fig. 4(b8)]. Therefore, we observed the MN3–C structure at $\lambda_b = 0.70$–0.95, which was slightly adjusted into the similar MN4–C structure [see Fig. 4(b9)]. We believe that the microstructure depends not only on the surface field and the confinement dimension but also is determined by surface curves and the periodic arrangement of cylindrical surfaces.

Hence, we investigated the morphological dependences on the strength of the surface field $\lambda_{a(b)}$ for arrays with other large nanorods of $D/L_0 = 1.91$, as shown in Fig. 5. For the degree of $D/L_0 = 1.91$, the rods occupy too much space in the array such that the inner structure is difficult to assemble in such a crowded area. Furthermore, it is easy to assemble the sphere-like (S) structure in the outer zone. For example, there is the S structure appearing in

the outer zone for the major blocks with the expectation of the unperfected lamella (UL1) structure, namely the UL1–S structure, occurring at $\lambda_a = 0$–0.45 [Fig. 5(a1)]. With increasing λ_a, the S structure disappears in the corner of the outer zone, instead of the emergence of the generic cylinders (GC) for the major-block component, resulting in the UL1–GC structure at $\lambda_a = 0.50$–1.00 [see Fig. 5(a2)]. For the B-block preferential surfaces, the diblock copolymers maintain the UL1–S structure at $\lambda_b = 0$–0.10 [Fig. 5(b1)] and subsequently develop into another UL2–S structure at $\lambda_b = 0.15$–0.55 [see Fig. 5(b2)]. When the strength of the surface field was increased to $\lambda_b = 0.60$–1.00, we observed an interesting structure, where quadrangular PAL are placed in rows at the four corners of calculation unit in the A-block domain, namely a quadrangular lamellar (QL) structure [see Fig. 5(b3)]. In these surface-induced processes, we observed discrete microstructures, including the S and GC structures in severe confinements, similar to cylindrical and spherical confinements where discrete microstructures also have been reported in severe confinements.[39,40,42,46,51,61]

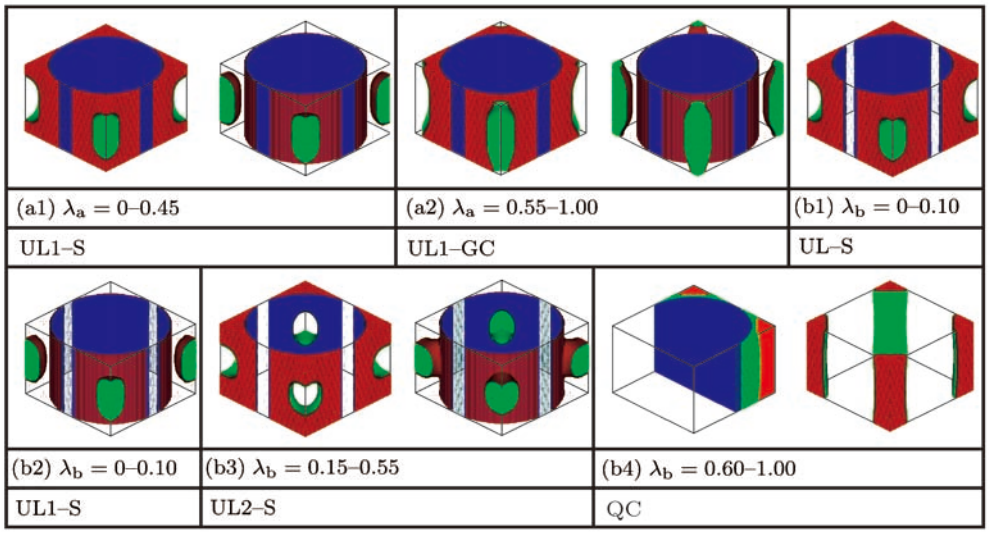


Fig. 5. Morphological dependences of lamella-forming diblock copolymers on the strength of surface field $\lambda_{a(b)}$ for the arrays with $D/L_0 = 1.91$. Here, The values of $\lambda_{a(b)}$ and denotations of morphologies are listed below the structures. The red, green and blue colours represent A-blocks, B-blocks and nanorods, respectively.

Several general characteristics of surface-induced morphologies of diblock copolymers can be summarized in arrays with large nanorods. On the one hand, the evolvements are relatively simpler than those observed in the arrays with small- or moderate-sized nanorods. In particular, there are a few microstructures which take part in evolvement at the surface in preference to minor blocks because of the hard wall effects. On the other hand, the morphologies have more cylindrical symmetries, such as the MN3–C, MN4–C and QC in arrays with large diameters and cylindrical structures prevail at strong surface fields, due to cylindrical symmetries originating from the surface fields.

4. Conclusion

In this article, we have reported results of SCFT calculations used to study the surface-induced effects on morphologies of the lamella-forming diblock copolymers in nanorod arrays. Not only did we increase the strength of the surface field by using small increments, but we also chose the model copolymers to be used as slightly asymmetric diblock copolymers, in which the equilibrium period is commensurate to the period of array. Taking advantage of this choice, we observed a rich variety of novel surface-induced morphologies of diblock copolymers confined in the nanorod arrays with different surface fields and several nanorod diameters.

Diblock copolymers exhibited distinguishing morphologies in arrays with weak and strong surface fields in the simulation study. For weak surface fields, we observed several bulk-like morphologies, such as the PAL, UPAL, and CPAL structures, in arrays with small nanorods, due to the small contact surfaces of nanorods. The transition sequences: CL–LN1, CL–LN2, and CL–LN1, CL–LN2, and DR–LN1, have been observed in arrays with moderate-sized nanorods for A- and B-preferential surfaces, respectively. This almost unchanged structure indicates that

the strong-ranged surface field is difficult to influence the structural evolvement in the outer zones in arrays with moderate-sized nanorods. For arrays with large nanorods, we observed novel morphologies, including CL–C, BCL–C, PEL, C, UL1–S, and UL2–S structures, in arrays with weak surface fields. The relatively fewer structures observed in such evolvements indicate that these structures are insensitive to the weak surface fields and that the diblock copolymers have relatively stable morphologies under such conditions. In addition, the diblock copolymers tend to assemble into the structures with cylindrical symmetries in arrays with strong surface fields. These structures include the BN3–C, CL–BN5, CL–BN6, CL–MN1–C, CL–C, CL–MN2–C, MN3–C, and MN4–C structures, as well as several cylinder-like structures, such as UL1–GC and QC structures. These structures with cylindrical symmetries basically originate from the strongly cylindrical symmetries of surface fields, especially of the surface fields with large contact areas.

In addition to the various strengths of surface fields, we also observed several distinguishing characteristics of surface-induced morphologies because of different preferential surfaces and various nanorod diameters in the simulation study. The diblock copolymers are obviously abundant in morphologies in arrays with moderate-sized nanorods, with varying strength of surface fields. The small and large nanorods provide either too small or too large contact surfaces that bring about simple evolvement processes. These results indicate that arrays with moderate-sized nanorods are suitable for offering confinement environments with a rich variety of self-assembled morphologies. Observations of A- and B-preferential surfaces showed that B-preferential surfaces more easily affect the morphologies of diblock copolymers, in which more novel structures were observed due to the majority blocks of copolymers. These observations on novel morphologies with outstanding characteristics may provide meaningful assistance for the fabrication of nanomaterials based on block copolymers.

References

[1] Soto-Figueroa C, Rodriguez-Hidalgo M R, Martinez-Magadan J M and Vicente L 2008 *Macromolecules* **41**(9) 3297

[2] Kim M I, Wakada T, Akasaka S, Nishitsuji S, Saijo K, Hasegawa H, Ito K and Takenaka M 2008 *Macromolecules* **41** 7667

[3] Takenaka M, Wakada T, Akasaka S, Nishitsuji S, Saijo K, Shimizu H, Kim M I and Hasegawa H 2007 *Macromolecules* **40** 4399

[4] Yoon J, Lee W and Thomas E L 2006 *Nano Lett.* **6** 2211

[5] Ruiz R, Kang H, Detcheverry F A, Dobisz E, Kercher D S, Albrecht T R, Pablo J J D and Nealey P F 2008 *Science* **321** 936

[6] Xiang H, Shin K, Kim T, Moon S, McCarthy T J and Russell T P 2005 *Polym. J. Sci.* Part B **43** 3377

[7] Huinink H P, van Dijk M A, Brokken-Zijp J C M and Sevink G J A 2001 *Macromolecules* **34** 5325

[8] Wang Q, Nealey P F and Pablo J J D 2001 *Macromolecules* **34** 3458

[9] Feng J, Liu H and Hu Y 2002 *Macromol. Theroy Simul.* **11** 556

[10] Podariu I and Chakrabarti A 2003 *J. Chem. Phys.* **118** 11249

[11] Wang Q, Nealey P F and Pablo J J D 2003 *Macromolecules* **36** 1731

[12] Xu T, Hawker C J and Russell T P 2005 *Macromolecules* **38** 2802

[13] Park I, Park S, Park H W, Chang T, Yang H and Ryu C Y 2006 *Macromolecules* **39** 315

[14] Tsarkova L, Knoll A, Krausch G and Magerle R 2006 *Macromolecules* **39** 3608

[15] Yin Y, Sun P, Jiang R, Li B, Jin Q, Ding D and Shi A C 2006 *J. Chem. Phys.* **124** 184708

[16] Alexander-Katz A and Fredrickson G H 2007 *Macromolecules* **40** 4075

[17] Heckmann M and Drossel B 2008 *Macromolecules* **41** 7679

[18] Heckmanna M and Drossel B 2008 *J. Chem. Phys.* **129** 214903

[19] Niihara K I, Sugimori H, Matsuwaki U, Hirato F, Morita H, Doi M, Masunaga H, Sasaki S and Jinnai H A 2008 *Macromolecules* **41** 9318

[20] Tan H, Song Q, Yang S, Yan D and Shi A C 2008 *Macromol. Theroy Simul.* **17** 45

[21] Park J H, Sun Y, Goldman Y E and Composto R J 2009 *Macromolecules* **42** 1017

[22] Shin C, Ryu D Y, Huh J, Kim J H and Kim K W 2009 *Macromolecules* **42** 2157

[23] Petrus P, Sal M L and Brennan J K 2010 *Langmuir.* **26** 3695

[24] Chen D, Gong Y, Huang H, He T and Zhang F 2007 *Macromolecules* **40** 6631

[25] Wang Q, Yan Q, Nealey P F and Pablo J J D 2000 *J. Chem. Phys.* **112** 450

[26] Wang Q 2005 *Macromol. Theroy Simul.* **14** 96

[27] He X, Song M, Liang H and Pan C 2001 *J. Chem. Phys.* **114** 10510

[28] Sevink G J A, Zvelindovsky A V, Fraaije J G E M and Huinink H P J 2001 *Chem. Phys.* **115** 8226

[29] Shin K, Xiang H, Moon S I, Kim T, McCarthy T J and Russel T P 2004 *Science* **306** 76

[30] Wu Y, Cheng G, Katsov K, Sides S, Wang J, Tang J, Fredrickson G H, Moskovits M and Stusky G D 2004 *Nat. Mater.* **3** 816

[31] Xiang H, Shin K, Kim T, Moon S I, McCarthy T J and Russell T P 2004 *Macromolecules* **37** 5660

[32] Xiang H, Shin K, Kim T and Moon S I 2005 *Macromolecules* **38** 1055

[33] Chen P, He X and Liang H 2006 *J. Chem. Phys.* **124** 104906

[34] Feng J, Liu H and Hu Y 2006 *Macromol. Theroy Simul.* **15** 674

[35] Feng J and Ruckenstein E 2006 *J. Chem. Phys.* **125** 164911
[36] Feng J and Ruckenstein E 2006 *Macromolecules* **39** 4899
[37] Li W and Wickham R A 2006 *Macromolecules* **39** 8492
[38] Li W, Wickham R A and Garbary R A 2006 *Macromolecules* **39** 806
[39] Yu B, Sun P, Chen T, Jin Q, Ding D, Li B and Shi A C 2006 *Phys. Rev. Lett.* **96** 138306
[40] Chen P, Liang H and Shi A C 2007 *Macromolecules* **40** 7329
[41] Wang Q 2007 *J. Chem. Phys.* **126** 024903
[42] Yu B, Sun P, Chen T, Jin Q, Ding D, Li B and Shi A C 2007 *J. Chem. Phys.* **127** 114906
[43] Sevink G J A and Zvelindovsky A V 2008 *J. Chem. Phys.* **128** 084901
[44] Yu B, Jin Q, Ding D, Li B and Shi A C 2008 *Macromolecules* **41** 4042
[45] Li S, Wang X, Zhang L, Liang H and Chen P 2009 *Polymer* **50** 5149
[46] Fraaije J G E M and Sevink G J A 2003 *Macromolecules* **36** 7891
[47] Arsenault A C and Rider D A 2005 *J. Am. Chem. Soc.* **127** 9954
[48] Yabu H, Higuchi T and Shimomura M 2005 *Adv. Mater.* **17** 2062
[49] Cheng J Y, Ross C A, Smith H I and Thomas E L 2006 *Adv. Mater.* **18** 2505
[50] Feng J, Liu H and Hua Y 2007 *Fluid Phase Equilibria* **261** 50
[51] Yu B, Li B, Jin Q, Ding D and Shi A C 2007 *Macromolecules* **40** 9133
[52] Chen P, Liang H and Shi A C 2008 *Macromolecules* **41** 8938
[53] Higuchi T, Tajima A, Motoyoshi K, Yabu H and Shimomura M 2008 *Chem. Int. Ed.* **47** 8044
[54] Li S, Chen P, Wang X, Zhang L and Liang H J 2009 *Chem. Phys.* **130** 014902
[55] Wang X, Li S, Chen P, Zhang L and Liang H 2009 *Polymer* **50** 4964
[56] Li S, Ji Y, Chen P, Zhang L and Liang H 2010 *Polymer* **51** 4994
[57] Fredrickson G H, Ganesan V and Drolet F 2002 *Macromolecules* **35** 16
[58] Drolet F and Fredrickson G H 1999 *Phys. Rev. Lett.* **83** 4317
[59] Liu M, Li S, Zhang L and Wang X 2010 *Chin. Phys.* B **19** 028101
[60] Yu B, Sun P, Chen T, Jin Q, Ding D, Li B and Shi A C 2007 *J. Chem. Phys.* **126** 204903
[61] Zhang Q 2009 *Chin. Phys.* B **18** 658